UC San Diego
UC San Diego Previously Published Works

Title

Deazapurine Nucleoside Analogues for the Treatment of Trichomonas vaginalis

Permalink

Journal

ACS Infectious Diseases, 7(6)

ISSN

2373-8227

Authors

Natto, Manal J
Hulpia, Fabian
Kalkman, Eric R
et al.

Publication Date

2021-06-11

DOI

10.1021/acsinfecdis.1c00075

Peer reviewed

Deazapurine nucleoside analogues for the treatment of *Trichomonas vaginalis*

Manal J. Natto[1,*], **Fabian Hulpia**[2,*], **Eric R. Kalkman**[1], **Susan Baillie**[1], **Amani Alhejeli**[1], **Yukiko Miyamoto**[3], **Lars Eckmann**[3,4], **Serge Van Calenbergh**[2], **Harry P. de Koning**[1,**]

[1.]Institute of Infection, Immunity and Inflammation, College of Medical, Veterinary and Life Sciences, University of Glasgow, Glasgow, UK

[2.]Laboratory for Medicinal Chemistry, Campus Heymans (FFW), Ghent University, Ottergemsesteenweg 460, B-9000 Gent, Belgium

[3.]Department of Medicine, University of California, San Diego, 9500 Gilman Drive, La Jolla, CA 92093, USA

[4.]Center for Discovery and Innovation in Parasitic Diseases, University of California, San Diego, 9500 Gilman Drive, La Jolla, CA 92093, USA

Abstract

Trichomoniasis is the most common non-viral, sexually transmitted disease in humans but treatment options are limited. Here, we report a Resorufin-based drug sensitivity assay for High Throughput microplate-based screening under hypoxic conditions. A 5203 compound Enamine kinase library and several specialized compound series were tested for inhibition of *Trichomonas* growth at 10 μM with Z' values >0.5. Hits were re-screened in serial dilution to establish an IC_{50} concentration. A series of 7-substituted 7-deazaadenosine analogues emerged as highly potent anti-*T. vaginalis* agents, with EC_{50} values in the low double digit nanomolar range. These analogues exhibited excellent selectivity indices. Follow-up medicinal chemistry efforts identified an optimal ribofuranose and C7 substituent. Several nucleosides rapidly cleared cultures of *T. vaginalis* at concentrations of just 2×EC_{50}. Preliminary *in vivo* evaluation in a murine trichomoniasis model (*Tritrichomonas foetus*) revealed promising activity upon topical administration, validating purine nucleoside analogues as a new class of antitrichomonal agents.

Graphical abstract

[**,]*Corresponding author*: **Harry P. de Koning** – Institute of Infection, Immunity and Inflammation, College of Medical, Veterinary and Life Sciences, University of Glasgow, Glasgow G12 8TA, UK; Phone: +44 (0)141 330 3753; harry.de-koning@glasgow.ac.uk.
[*.]These authors contributed equally

Author contributions

MJN and FH contributed equally.
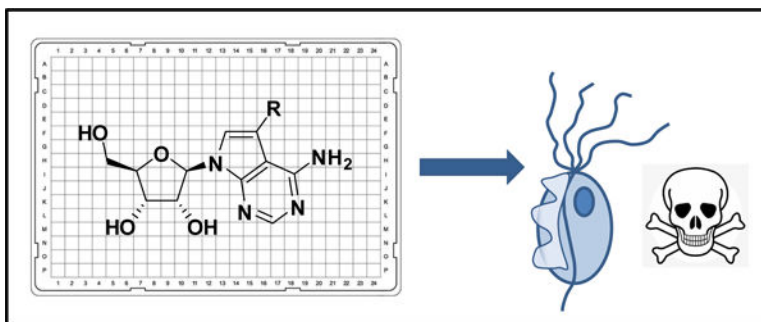
Lay summary:

Trichomoniasis is one of the most common sexually-transmitted infections in humans, with an estimated 300 million cases world-wide; it is caused by the single-celled protozoan parasite *Trichomonas vaginalis*. Currently, only two, closely related drugs are available as treatments and resistance to both is being reported, making new drug development a priority. Here, we report the adaptation of an existing drug testing method for high-throughput screening. The screening effort led to the discovery of a class of adenosine analogues as potent new anti-trichomonal agents. The structure was systematically optimised using medicinal chemistry and showed that 7-phenyl 7-deazaadenosines have the best combination of activity against the parasite and low toxicity against a human cell line. The effect of these compounds on *T. vaginalis* appeared to be irreversible and affected cell division. Importantly, the lead compound cured a mouse model of trichomoniasis. The new compound series has significant potential for preclinical development.

Keywords

Trichomonas vaginalis ; nucleoside analog; high-throughput screening; tubercidin; mouse model

Trichomoniasis is considered to be the most common non-viral sexually transmitted infection (STI) worldwide, with an estimated annual incidence of 300 million cases.[1–3] Despite this, trichomoniasis has been largely overlooked compared with other STIs such as HIV and gonorrhoea, as evidenced by a lack of routine screening programmes and a poor understanding of the true burden of disease. Trichomoniasis typically affects patients between 15 and 49 years old, and is more prevalent among people with low income, multiple sexual partners, or concomitant genital disease.[4]

Historically, trichomoniasis has been regarded as a clinically mild infection, often asymptomatic in males and causing only 'nuisance' symptoms in females (for example, inflammation of the vaginal area and pain during urination and intercourse). Nevertheless, trichomoniasis can lead to serious complications, including an increased risk of pelvic inflammatory disease and infertility, as well as increased susceptibility to cervical and prostate cancer, benign prostatic hyperplasia, and increased risk of HIV infection.[5–9] In pregnant women, trichomonal infection is associated with an increased risk of preterm birth, premature rupture of membranes, and below-average infant birth weight.[10, 11]

Trichomoniasis is caused by *Trichomonas vaginalis*, an anaerobic protozoan parasite for which humans are the only natural hosts. The parasite takes the form of a free-swimming trophozoite, with four anterior flagella to aid motility and a fifth flagellum attached to an undulating membrane to assist movement.[2] *T. vaginalis*, being anaerobic, does not possess mitochondria. Instead, energy is provided through fermentative carbohydrate metabolism by multiple hydrogenosomes, a key morphological feature and target for antiparasitic treatment.[12]

T. vaginalis infection is passed on during sexual intercourse through vaginal or prostatic secretions. Infection of a new host begins in the lower genital tract, where the parasite preferentially binds to the vaginal epithelium in females, and epithelial cells in the urethra and prostate in males.[13] Once binding occurs, the typical pyriform shape of the parasite differentiates to an amoeboid shape, increasing contact with the epithelial cell surface; exosomes containing *T. vaginalis* proteins and RNA play a vital role in the host-parasite interactions.[1,6] *T. vaginalis* also releases polyamine metabolites, such as putrescine, resulting in cell damage and, in *in vitro* experiments, cell apoptosis.[14] The host inflammatory response is countered through phagocytosis, supplying the parasite with nutrients not only from epithelial cells but also lactobacilli, leukocytes and, most importantly, iron-rich erythrocytes released after inducing vaginal bleeding, promoting survival.[15, 16]

Curative treatment options for trichomoniasis are limited to two members of a single class of antimicrobials, the 5-nitroimidazoles metronidazole and tinidazole.[2,17] These drugs enter the *T. vaginalis* hydrogenosomes by passive diffusion.[18] They are believed to be anaerobically reduced and kill *T. vaginalis* through the production of free radicals and toxic metabolites.[18, 19]

Metronidazole is usually the first-line treatment and is highly effective in most cases.[19] However, the development of *T. vaginalis* resistance to nitroimidazoles is a growing problem, with up to 5% of clinical cases of vaginal trichomoniasis being associated with *T. vaginalis* strains with some nitroimidazole resistance.[1,20,21] Currently, the only treatment for nitroimidazole resistant trichomoniasis is a higher dose of the same drug, but this are poorly tolerated.[19,21] Considering the cross-resistance between metronidazole and tinidazole, and the reported therapeutic failure of both,[22] there is an urgent need to develop new therapeutics with a novel mechanism of action.

New drug development for trichomoniasis has been largely held back by the perceived sufficiency of cheap metronidazole, and the interest in the discovery of new lead compounds to treat trichomoniasis has also been hampered by the lack of suitable screening assays. Very recently, an image analysis-based high content assay for drug screening against *T. vaginalis* was published and, although very reliable, it requires specialised equipment, fixation of the cells and dual staining with two fluorophores.[23] We have previously reported that the resazurin ('Alamar blue') assay, which had been proposed by some researchers[24,25] is not suitable for *T. vaginalis* as the ascorbic acid present in the culture medium is also capable of reducing resazurin to resorufin, even in the absence of live cells, giving a very high, time-dependent background fluorescence.[26] However, live cells are required for the reduction of resorufin to dihydroresorufin, and *Trichomonas* is one of few cell types with the reductive

potential required. This makes a resorufin-based assay, based on diminishing fluorescence proportional to cell numbers, highly specific.[27]

Here, we scale-up and validate this assay for high-throughput usage, while evaluating several sets of compounds for anti-trichomonad activity, including a commercial library of protein kinase inhibitors and a smaller series of 7-deazanucleoside analogues that had already produced lead compounds for other parasitic diseases, especially Chagas disease and sleeping sickness.[28–30] We employed stringent hit criteria of better performance than 1 μM metronidazole (EC$_{50}$ ~0.3 μM) at 10 μM of test compound, which identified multiple nucleoside analogues with EC$_{50}$ values superior to metronidazole and low toxicity to Human Embryonic Kidney (HEK293) cells. Medicinal chemistry exploration provided clear structure-activity relationship trends for the sugar ring as well as the 7-position substitution. Selected analogues were shown to exhibit *in vitro* cidal character against the parasite. Finally, the *in vivo* potential of purine nucleoside analogues was demonstrated in a mouse model of trichomoniasis.

MATERIALS AND METHODS

Trichomonas vaginalis cultures

T. vaginalis trophozoites of the metronidazole-sensitive strain G3 (kind gift of Professor Jeremy Mottram, University of York, UK) were grown *in vitro* in modified Diamond's media (MDM) with 10% heat inactivated horse serum (HIHS; Gibco Life Technologies), pH adjusted to 6.3 – 6.4 (Natto et al, 2015). MDM composition was 20 g/L trypticase peptone (BD Biosciences, Sparks, USA), 10 g/L yeast extract (Formedium Ltd, UK), 5 g/L of maltose monohydrate (Sigma, UK), 1 g/L L-ascorbic acid (Sigma), 1 g/L KCl, 1 g/L KHCO$_3$, 1 g/L KH$_2$PO$_4$, 0.5 g/L K$_2$HPO$_4$ and 0.1 g/L FeSO$_4$.2H$_2$O.[26] Trophozoites were seeded at ~1×10^5 cells/mL in 25-mL Universal bottles that were completely filled, tightly capped to maintain an anaerobic environment, and cultured for 24 h at 37 °C before passage at ~1×10^6 cells/mL. Cell densities were determined microscopically by haemocytometer (Camlab, Cambridge, UK), or using a Beckman Coulter Z2 Particle Counter.

Optimisation of the resorufin-based assay

The resorufin-based assay was performed essentially as reported previously[27] but with several amendments to improve reproducibility and throughput. The assay was performed in white 384-well plates rather than 96-well plates, and a multi-drop reagent dispenser (Thermo Multidrop Combi, ThermoFisher Scientific, UK) was used for the addition of *Trichomonas* trophozoites (final density 5×10^4 cells/mL in standard medium) and of 20 μL resorufin 0.5 μM in PBS) to the test plates. Anaerobic incubation of cells with test compounds was for 24 h, and an additional period of 2 h after the addition of the resorufin. The incubations were performed in an airtight pod (StoragePod®, Roylan Developments Ltd, UK) flushed with 98% N$_2$/2% O$_2$ and placed inside a 37 °C incubator, allowing strict atmospheric and temperature control as well as incubation of the resorufin without light, which has been shown to limit its efficacy.[31]

Validation for high-throughput screening

The optimised assay was validated for high-throughput screening applications using the 5203-compound Enamine Kinase Library, designed and synthesised by Enamine Ltd (Ukraine) with a special focus on potential novel protein kinase inhibitors. Compounds were acquired as 10 mM solutions in 100% DMSO, pre-diluted and stamped to 384-well assay plates (Greiner Bio-One, Germany) in batches (Figure S1A). The original stocks were 10-fold diluted to 1 mM in 100% DMSO ('motherplates'), from which 'daughterplates' were stamped at 100 μM in PBS followed by the final 10-fold dilution for an in-assay concentration of 10 μM. The first batch was run as seven families (14 plates) and the second as 10 families (20 plates), allowing a day in between for reading the first batch. Each batch included a control-only Masterblock deep-well plate (Greiner Bio-One) made at 100 μL (10× in assay concentration), with only columns 1, 2, 23 and 24 filled; the remaining wells were filled with 5% DMSO.

For the other compound series, stock solutions were prepared for each compound from dry powder provided. Compounds were dissolved in DMSO to create 20 mM stock solutions, which was aliquoted into Eppendorf tubes to prevent repeated freezing and thawing from affecting the activity of the compound. Metronidazole (Sigma), acting as a positive control, was also prepared as a 20 mM solution in DMSO.

T. vaginalis cultures were seeded into the pre-dispensed assay plates at a final density of 5×10^4 cells/mL using the multi-drop dispenser. All liquid handling regarding the compound library was performed on a Biomek FX[P] robotic platform (Beckman Coulter Inc., USA). Compound dilution plates were generated in PBS (pH 7.4), leaving the outer two columns on either side empty for controls (Figure S1). Instead of a single positive control concentration, a serial dilution control of metronidazole was set up in column 1. A 0.5% DMSO vehicle control was used as a negative control to obtain a vehicle control signal that should not interfere with measuring fluorescence reduction.

Assay plates were prepared in duplicate, one set for use with the BD pouch bag method as described[26] and the other set for use with the pod. The pod was first purged to 2% O_2 with 100% N_2 from a cylinder (BOC Industrial Gases UK). Plates were sealed with breathable seals and stacked, with spacers to allow free air circulation between the plates, in order to negate any potential difference in top-to-bottom gas exchange within the pod. In-pod evaporation was limited by the addition of several water reservoirs within the pod. The pod containing the assay plates was then placed into a regular incubator at 37 °C. After 24 hours, 0.5 μM resorufin sodium salt (Sigma) in PBS was added to the plate (10 μL per well using small cassette) by multi-drop dispenser. The plates were replaced inside the pod, with 2% O_2/98% N_2 atmosphere and incubated again at 37 ºC.

After 2 h, fluorescence readouts were obtained using a BMG PHERAstar® FS plate reader (BMG Labtech, UK), using an excitation wavelength of 544 nm and an emission wavelength of 620 nm. All plates were normalised to the average vehicle control signal and the Z' factor was calculated for each plate to evaluate the robustness of the data. The formula used was $Z' = 1 - 3((\delta_{pos} + \delta_{neg}) / (\mu_{pos} - \mu_{neg}))$, where δ_{pos} is the standard deviation for the metronidazole control, δ_{neg} is the standard deviation for the vehicle control, μ_{pos} is the mean

signal for the metronidazole control and μ_{neg} is the mean signal for the vehicle control. Hit compounds from plates with a Z' > 0.5 were re-screened in a follow-up assay (Figure S1B). Hits were taken as compounds associated with a higher level of resorufin fluorescence than control wells with 1 μM metronidazole.

A small purine nucleoside library was screened separately. These small screen assays were performed in 96-well plates (Greiner Bio-One, Germany) using 6-, 12- and 24-well doubling dilution series starting at 200 μM test compound (diluted from 20 mM stock in DMSO), with duplicates on a single plate. 100 μL of MDM media was added to each well of the plate using a multi-channel pipette, leaving only the first well empty, to which 200 μL of compound in MDM media was added at a double the final concentration of 100 μM. Doubling dilution of the compounds were performed by mixing 100 μL from the first well with the media in the second well, and repeating the action across the plate. Care was taken to ensure that the solution was well mixed by pipetting up and down 10 times in each well. The last well was left drug-free to act as a negative control.

A *Trichomonas* culture was diluted with media to 5×10^5 cells/mL and 100 μL of the solution added to all wells by multi-drop dispenser (ThermoFisher Scientific, UK) contained within a sterile robotics enclosure (Bigneat Contaminant Technologies, Worldwide). The plates were inserted into the StoragePod enclosure and incubated for 24 h (2% O_2/98% N_2, 37 ℃), followed by the addition of 30 μL 0.5 mM resorufin solution using the multi-drop dispenser and further anaerobic incubation in the pod for 2 h before obtaining the fluorescence readout as above. For the adenosine analogue compound set, mean ± standard deviation EC_{50} was calculated from nine repeats using non-linear regression (equation for sigmoidal curve with variable slope; GraphPad Prism 6). For the other sets, EC_{50} values were averaged over three repeats. Partial inhibition curves were extrapolated for EC_{50} with bottom values defined by the positive control, but only if more than half of the curve was obtained.

Growth curves

Cultures to assess impact on growth rates and survival were seeded at 2×10^5 cells/mL in 6-well culture plates (Greiner Bio-One, Germany) for several of the most active compounds identified in the resorufin drug-sensitivity assay, at $2 \times EC_{50}$ concentration, and incubated under microaerobic conditions at 37 ℃. At 8-h intervals samples were taken from each well for cell counts, using a Beckman Z Series Coulter Counter, and for fluorescence microscopy after staining with 4′,6-diamidino-2-phenylindole (DAPI (Vector Laboratories, Burlingame)). Due to the rapid growth of the control (no drug) culture, cultures were passaged after 24 h, back to 1.32×10^5 cells/mL, in fresh medium. Metronidazole was used as a positive control and untreated cells were used as a negative control.

Fluorescence microscopy

To prepare slides for fluorescence microscopy, cell samples taken during the growth curve experiment were centrifuged at $2600 \times g$ for 10 min at 4 ℃. The cell pellet was resuspended in 1× PBS pH 7.4, centrifuged again for 10 min at $2600 \times g$ and re-suspended in sterile PBS, of which 50 μL was applied to microscope slides (Thermo Scientific, UK) coated with poly-L-lysine (Sigma, UK), allowed to air dry in the sterile hood for 30 min, fixed for 15

minutes in 4% paraformaldehyde/PBS and then washed twice with 1 mL PBS. This was blotted off, the slides air-dried but not completely. A drop of Vectashield anti-fade mounting medium with DAPI (Vector Laboratories) was added to the slides and spread by a coverslip (CamLab); coverslips were sealed with clear nail polish. Slides were observed for cell morphology under an Axioskop microscope (Image Solutions, Preston, UK) using softWoRx software, while DNA configuration was assessed using a Zeiss Axioplan fluorescence microscope using Hamamatso digital camera and Openlab software. For detailed observation of single DAPI-stained cells and the measurement of nuclear volumes, Z-stacks of DAPI-stained cells and subsequent data analysis, FIJI software[32] and/or IMARIS (Bitplane) was used.

Nucleoside analogues

Purine nucleoside analogues were prepared as previously reported.[28,30] Synthesis and spectral characterization of newly synthesized analogues evaluated in this study, is presented in the Supporting Information.

In vivo assay

Breeding pairs of BALB/c mice (originally obtained from Jackson Labs) were maintained in the UC San Diego animal facility. Freshly weaned (21–24 days) females were used for the studies. Animals were housed at a constant temperature room (22 ± 1 °C) with a 12 h light/ 12 h dark cycle and provided access to food and water ad libitum. All animal studies were reviewed and approved under protocol number S00205 by the UC San Diego Institutional Animal Care and Use Committee. For drug efficacy studies, *T. foetus* D1 trophozoites were grown to mid-logarithmic phase, and intravaginally inoculated (10^6 in a 5 μL volume in growth medium) into weanling mice. After one day, mice were either treated with five doses over three days of drug suspension in 1% hypromellose by oral gavage (50 μL, 25 mg TH1012/kg per dose) or topically by intravaginal injection of (5 μL, 50 μg TH1012 or solvent control per dose), five doses over three days (1 x dose on day 1; 2 x doses each on days 2 and 3). Live trophozoites were enumerated in a counting chamber on day 4 in vaginal washes of 30 μL of PBS.[33]

RESULTS

Validation of the resorufin-based assay

Although we have reported on the development of a resorufin assay for drug screening against *T. vaginalis* before,[26] we sought to improve its dynamic range, cost per sample, scale and reproducibility by improving culture conditions and adapting to 386-well plates with automated liquid handling. We first verified that the incubation of *T. vaginalis* in the atmosphere-controlled pod gave the same reliable results as our previously published incubations in an anaerobic pouch bag (BD Bioscience, San Jose, CA). The resorufin signal was strongly correlated with cell density using either incubation method, but the best correlation, over the longest dilution range, was achieved with the pod, with a correlation coefficient of 0.983 over a dilution range spanning more than 5 orders of magnitude (50.9 cells/mL - 6.67×10^6 cells/mL), while the fluorescence became non-linear with pouch bag-grown cells above a density of 4.17×10^5 cells/mL (Figure 1A). In a test run with 16 repeats

a doubling dilution series with the positive control metronidazole (21 doubling dilutions plus no-drug control), the EC_{50} values obtained were not statistically different for the two methods (0.28 ± 0.02 μM and 0.26 ± 0.02 μM for the pod and for the pouch bags, respectively; n=16, *P*=0.58 by unpaired t-test) (Figure 1B).

Initial hit-identifying screen with multiple compound series

The primary screen used a number of medium and small compound libraries, including a 5203 compound Enamine Kinase library, and the following smaller libraries that included compounds that had previously shown activity against other protozoa. These included twenty 1-(4-Methane(amino)sulfonylphenyl)-3-(4-substituted-phenyl)-5-(4-trifluoromethylphenyl)-1H-2-pyrazolines/pyrazoles,[34] 20 coumarin and bi-coumarin compounds,[35,36] 8 triarylpyrazolines,[37] 10 aminosteroids isolated from the West African shrub *Holarrhena africana*,[38] 33 5'-norcarbocyclic pyrimidine nucleosides,[39,40] and a series of 18 7-subsituted 7-deazaadenosine analogues that we had previously prepared and profiled against kinetoplastid parasites.[28–30] All compounds were tested at a single concentration of 10 μM and initial hits were defined as fluorescence higher than the average fluorescence in the presence of 1 μM metronidazole; all pates displayed Z' factors ranging from 0.5 to 0.92.

Using these criteria, 25 initial hits were identified from the kinase inhibitor library (some of them performing only marginally better than 1 μM metronidazole), of which two were clearly confirmed in a re-screen but both contained reactive maleimide groups and were dismissed as pan-assay interference (PAINs) compounds.[41,42] None of the other compound series produced hits in the initial single concentration screen with these criteria, except the 7-substituted 7-deazaadenosine analogue series, which produced several clear hits. Therefore, this series was run in a secondary assay with 23 dilutions and no-drug control, producing EC_{50} values ranging from 0.029 to 8.3 μM (Figure 2).

Structure-activity investigation of 7-substituted 7-deazaadenosine analogues against T. vaginalis

Given the promising activities of the deazaadenosines in the library screens, we focused on these compounds for further activity explorations. Confirmation experiments revealed that all assayed analogues displayed strong *in vitro* activities, with EC_{50} values ranging from low micromolar for the 3'-deoxyribofuranoses FH8480, FH8481 and FH10680, to double-digit nanomolar EC_{50} values for ribofuranoses TH1011, TH1012 and FH3147 (Figure 2 and Table 1). Indeed, all 6 ribofuranoses, two of the 3'-deoxyfuranoses and two of the 2'-deoxy analogues displayed EC_{50} values lower than that of metronidazole (EC_{50} 0.53 ± 0.10, n=9). The highest activity was found for analogue FH3147 (7-deaza,7-(3,4-dichlorophenyl)adenosine), with an EC_{50} of 0.029 ± 0.001 μM (n=9), 18.3-fold more active than metronidazole (P<0.001, unpaired t-test).

Matched pair analysis showed that the ribofuranose nucleoside analogues generally elicited superior anti-*T. vaginalis* activity over their 3'-deoxy and 2'-deoxy congeners (Figure 2). Linear regression analysis showed significant correlation between the EC_{50} sets of the ribofuranose nucleosides and the 3'-deoxy and 2'-deoxy datasets ($r^2 = 0.67$ and 0.97,

respectively), with significantly non-zero slopes ($P = 0.047$ and 0.0004, respectively; F-test) (Figure S3). This analysis clearly established an EC_{50} ranking ribofuranose $\ll$ 2'-ribofuranose 3-deoxyribofuranose, with FH8494 as an outlying exception. This observation seems to suggest that most of the nucleoside analogues could act similarly on the parasite but with different efficacy depending on the presence or absence of the 2' and 3' hydroxyl groups.

Regarding the substitution pattern on the phenyl ring in this initial subset, electron-withdrawing and lipophilic substituents resulted in the most potent analogues, mimicking the SAR trends that were observed for *T. cruzi*.[28,30] However, we hypothesized that the lipophilic character of the 4-substituent on the phenyl ring likely plays the greater role for the antiparasitic activity against *T. vaginalis* (as compared to the reported anti-*T. cruzi* activity,28,30 given that the difference between 4-Cl and 4-Me substituents is relatively small (except for the 3'-deoxyribofuranose series). The effects on the phenyl ring substitutions on activity in all three series converged to the same findings, reinforcing the hypothesis that the ribofuranose modifications modulate the activity rather than elicit a different mechanism of action.

Exploration of the structural determinants for anti-trichomonal activity

We next investigated the structure-activity relationship of the best hits. Based on the observed weaker activity trend of the 2'-deoxyribofuranose analogues compared to their 3'-deoxyribofuranose and particularly ribofuranose matched-pair analogues, the 2'-deoxyribofuranose series was not further pursued. Thus, the test series was extended with previously prepared 3'-deoxyribofunarose[28] and ribofuranose[30] derivatives (Figure 3A) as well as 29 newly synthesized ribofuranose analogues, which allowed creating a suitable matched pair set.

We observed that activity of the 7-deaza-7-phenyladenosine (TH1004) and its 3'-deoxy congener (FH8480) improved upon introduction of a *para*-methyl or a *para*-chloro substituents, which have positive π values, but opposing σ values Figure 3A and Table 1. In the ribo-series the *para*-CF$_3$ and *para*-OCF$_3$ phenyl analogues were less potent than the para-methyl analogue (TH1011). The *para*-Et analogue (FH11702) also displayed weaker activity than the *para*-methyl analogue (TH1011). In both the ribo and the 3'-deoxyribo series, introduction of electron-withdrawing ($+\sigma$) and polar ($-\pi$) substituents (CN, CONH$_2$ and SO$_2$Me) led to a severe loss of antitrichomonal activity. Remarkably, the *para*-hydroxy substituted FH13833 displayed potent *in vitro* activity, possibly pointing to its engagement in a H-bonding interaction with a transporter or target protein.

The need for an aromatic substituent at C-7 was demonstrated by the cyclohexen-2-yl (FH10667) and cyclohexyl (FH10669) analogues, which exhibited very weak activity. Translocation of the most promising substituents to the *meta* and *ortho* positions, indicated that, at least for Cl and Me groups, *para* substitution is preferred, with the order being *para* > *meta* > *ortho*. Interestingly, in the fluorophenyl series the *ortho*-substituted analogue (FH7435) outperformed its *meta* isomer.

In general, the previously observed trend of ribofuranose analogues being more potent than their 3'-deoxy counterparts, was confirmed, except for 7-trifluoromethoxyphenyl substituted analogues FH10715 and FH9577.

Next, we investigated a subset of differently di-substituted phenyl analogues (Figure 3B). We started by replacing the 3-chloro group of the most potent analogue FH3147 and its 3'-deoxy congener FH8513 to a methyl (FH11705/FH10648), fluoro (FH10714/FH10683), trifluoromethyl (FH13827) and methoxy group (FH10649) and further expanded the series with 3-Cl, 4-F (FH11707/FH10681), 3,4-F$_2$ (FH11706/FH10682), 3-Cl, 4-CF$_3$ (FH13825) and 3-Cl, 4-OMe (FH10645) motifs.

The addition of a methyl group in the 3-position of TH1012/FH8512 resulted in a slight activity drop. The addition of a 3-chloro to TH1011/FH8481 resulted in equipotent (FH11703 versus TH1011) or slightly improved activity (FH10644 versus FH8481). All other di-substituted analogues showed at least 4-fold higher EC$_{50}$ values than TH1012, but most retained submicromolar EC$_{50}$ values.

Given the notable activity of the 2-fluorophenyl analogue FH7435, a 2-fluoro group was combined with a 4-Cl (FH13823) and 4-Me substituent (FH13824). The 2-F, 4-Cl analogue was equipotent with its 4-Cl parent TH1012, while the 2-F, 4-Me analogue approached the activity of its 2-F parent. The 2-naphthyl–substituted analoguesFH8461 and FH9575 showed reduced activity, compared to the 3,4-dichlorophenyl analogues FH3147 and FH8513, indicating that the fused phenyl ring is too large to be accommodated. Finally, we also validated the importance of the 4-Cl in these di-substituted analogues, by preparing 3,5-di-substituted analogues 3-Cl, 5-Cl (FH8460/FH10642) and 3-Cl, 5-Me (FH13830), which, showed a steep drop in activity.

A final subset of 7-heterocycle substituted nucleosides,[30] (Figure S4) displayed weaker activity than the corresponding phenyl or 4-Cl-phenyl analogue, strengthening the notion that a (substituted) phenyl ring is the preferred pharmacophore for the 7-position.

Growth curve assay

A growth curve assay was performed over a 56-hour period of continuous exposure to test compounds at a concentration of 2×EC$_{50}$, with cell count readings taken every 8 hours for this duration; metronidazole was used as a positive control and untreated cells as a negative control. The experiment was performed for 18 of the active compounds and the growth effects essentially separated into two different responses. Most displayed a rapid inhibition of growth, or cell death, which was highly evident even at the first 8 h time point. There was no recovery after passage with readjusting to $1.3×10^5$ cells/mL in fresh medium with the same concentration of drug after 24 h. Figure 4A shows selected matched pairs of ribofuranose and 3'-deoxy ribofuranose analogues. The ribofuranose analogues appeared to act faster but otherwise very similar to the corresponding 3'-deoxy compounds and completely depressed *T. vaginalis* growth over the course of the experiment, consistent with a similar mode of action, which appeared to inflict irreversible damage on the cells. In contrast, cells incubated with 2× EC$_{50}$ concentrations of 4-CF$_3$ or 4-OCF$_3$-substituted derivatives displayed continued albeit somewhat reduced growth over at least the first 24 h

(Figure 4B), and after treatment with the 4-OCF$_3$ analogue, growth resumed in fresh media. It thus appears that the halogenated phenyl analogues and the (O)CF$_3$-substituted analogues display different actions on the cell.

Assessment of in vitro toxicity on mammalian cell lines

Here we report the systematic testing of almost all the derivatives for toxicity against Human Embryonic Kidney (HEK) cells, except for a number of low activity derivatives. Table 1 shows all the EC$_{50}$ values against *T. vaginalis* and HEK cells side by side, along with the Selectivity Index (SI). Most of the test compounds displayed less than 50% inhibition of HEK cell growth at 200 μM, resulting in excellent SI values for most, including seven ribofuranose analogues and one 3'-deoxyribofuranose analogue with SI >1000. Some of the analogues were previously also assayed on human MRC-5 fibroblasts[28,30] but none were found to elicit significant cytotoxicity towards this cell line.

Fluorescence imaging

In order to have a preliminary assessment of whether defects in the cell division cycle might be responsible for the irreversible growth arrest and cell death observed, slides for fluorescence microscopy, treated with the DNA stain DAPI were prepared in tandem with the growth curve experiment at 8-h intervals until the 48 h point. Nuclei of fixed cells were stained using DAPI. When compared to the negative control of untreated cells at 24 h, cells treated with the adenosine analogues exhibit some notable morphological changes (Figure 5). In cells treated with compound TH1004, the cell membrane appears to be disintegrating and multiple nuclei are present in some cells, which differ from the two nuclei distinctively seen in dividing cells at 16 h of incubation. Similarly, cells treated with TH1012 also displayed multiple nuclei at 24 h, and the cells seem to have taken on a more rounded aspect - a trend that already started at 16 h. The cells treated with 4-OCF$_3$ derivative FH9577, in contrast, looked healthy at 16 h. Yet, these cells also clearly displayed multiple nuclei at 24 h. The multinucleate appearance could be due to nuclear fragmentation or to a cell cycle defect interfering with cytokinesis resulting ultimately in cells with usual numbers of nuclei per cell. Since there was a certain uniformity in the cells at 24 h, with many swollen cells with three or four apparent nuclei, the latter possibility appears to be more likely.

The promising results obtained *in vitro* against the parasite as well as the low levels of cytotoxicity found against the HEK cells, instigated us to further explore the potential of one analogue in a mouse model.

Activity of TH1012 against T. foetus in vitro and in vivo

We next investigated the *in vivo* efficacy of the most promising compounds in a murine model of vaginal trichomonad infection. Although mouse models of *T. vaginalis* have been reported,[43,44] they are generally less suitable for drug testing. Instead, we employed an infection model with the related trichomonad, *T. foetus*. First, TH1012, one of the most active hits against *T. vaginalis*, was tested against *T. foetus* strain D1 *in vitro*. We observed an EC$_{50}$ value of 13.9 μM (compared to *T. vaginalis* strain F1623 EC$_{50}$ of 0.18 μM in the same assay). Next, weanling BALB/c mice were inoculated intravaginally with *T. foetus* trophozoites to establish infection. After one day, mice were treated five times, either

with 25 mg/kg TH1012 orally, or intravaginally (Topical, 1%). Infected mice given solvent alone served as the control. Live trophozoites were obtained through vaginal washes and enumerated. Topical treatment led to almost complete eradication of the infection (Fig. 6). Administration of compounds by the oral route was less effective, showing only a modest ~7-fold decrease in trophozoite counts which did not reach significance relative to the solvent controls (Fig. 6). No adverse effects were observed during the treatment period.

DISCUSSION

In this investigation, we aimed to further optimise the published protocol for the resorufin-based assay previously adapted from the Alamar blue (Resazurin) assay,[26] to make it more applicable to large-scale drug screening, while still keeping it easy to operate with few steps and relatively inexpensive equipment. The development of a protocol that is suited to the screening of large compound libraries was seen as highly important due to the urgent need for new treatments. Improvements to our previously published protocol,[27] including optimised liquid handling and micro-aerobic incubation conditions were implemented and validated by the reproducibility, side-by-side comparisons and Z' values. Although a high content assay for *T. vaginalis* was recently described, and that assay appears to be suitable for HTS,[23] we believe that our protocol has the merit of being simpler and cheaper as it does not require expensive equipment beyond automated liquid handling (preferably) and a fluorescence plate reader. In the high-content assay it is necessary to fix the cells with glutaraldehyde and apply two stains to distinguish between the live and dead cells. In contrast, our method requires only the addition of resorufin to live cells, followed by a short incubation under standard growth conditions.

Having validated the optimised assay over a cell density range of ~5.5 log units, we used the revised protocol to evaluate the antitrichomonal activity of a number of compounds belonging to different classes. All validated hit compounds originated from the adenosine analogue series. The lack of efficacy observed with the LN series of 5'-norcarbocyclic uridine analogues is consistent with a study that reported little or no inhibition of *T. vaginalis* growth with modified uridine analogues but that same study did identify some adenosine analogues, including adenine arabinoside, 2'-F,2'-deoxyadenosine 2'-deoxy-2'-fluoroarabinoadenosine, with substantial antitrichomonal efficacy.[45] In addition, it was shown that 2-F, 2'-deoxyadenosine is a substrate of the *T. vaginalis* purine nucleoside phosphorylase (TvPNP), resulting in the generation of 2-F-adenine. These two compounds both possess antitrichomonal activity around the 100 nM mark.[46]

Consistent with the higher efficacy of adenosine analogues over uridine nucleosides, adenosine is taken up much more efficiently by *T. vaginalis* than uridine,[47] although the parasite is equally auxotrophic for purines and pyrimidines.[48]

Our extensive follow-on from the initial 7-aryl-7-deazaadenosine hits TH1012 and FH3147 showed that the SAR was surprisingly broad within the confines of 7-aryl substituted tubercidins, in that submicromolar activities were achieved with ribofuranoses, 2'-deoxyfuranoses and 3'-deoxyfyuranoses, as well as with mono- and di-substituted 7-aryl

moieties, with halogen, methyl, ethyl and methoxy substitutions often on positions 3 or 4 or both.

According to Munagala and Wang,[49] *T. vaginalis* either metabolises adenosine to guanosine nucleotides via adenosine deaminase, purine nucleoside kinase, IMP dehydrogenase and GMP synthase, or to adenosine nucleotides via an adenosine kinase. Of the two, it seems more plausible that the 7-substituted tubercidins would be phosphorylated in one step to yield the corresponding 5'-monophosphate analogue, rather than in four steps to the respective GMP derivative, especially given the broad SAR which all four enzymes would have to accommodate. Moreover, 3'-deoxytubercidin was previously found to be a substrate of *T. brucei* adenosine kinase.[29] According to the Munagala and Wang model, adenosine kinase is an essential enzyme in *T. vaginalis*, it being the only route for adenosine into the nucleotide pool. We thus hypothesise that the anti-trichomonal adenosine analogues exert their activity either as inhibitors or as subversive substrates of the essential enzyme adenosine kinase.

Lead compound TH1012 was used *in vivo* via oral and topical administration at substantial dosage without any apparent ill effects on the animals, as was the case when TH1012 and FH8512 were previously used in mouse models of Chagas' disease.[28] The topical administration of TH1012 almost completely eradicated the *T. foetus* infection. These observations show the lead compounds to be highly selective *in vivo* as well.

The effects of some of the adenosine analogues on *T. vaginalis* growth and cell cycle was studied and it was found that ribofuranoses acted fastest, with almost immediate growth arrest, whereas cells treated with the matching 3'-deoxyfuranoses (or metronidazole) managed a modest amount of growth before arrest and population decline. This may simply reflect the relative rate of uptake of ribofuranoses and 3'-deoxyribofuranoses but could equally reflect a difference between inhibition of, or conversion by, adenosine kinase. Addressing the metabolism and uptake of the identified leads will be a key priority in taking these compounds towards potential development. An exception to the observed rapid growth arrest was found with 4-CF_3-phenyl or 4-OCF_3-phenyl substituted tubercidins, which displayed substantial levels of growth up to 24 h, and whose effects were at least partially reversible. Nucleic acid staining with DAPI of samples taken at 16 h and 24 h of the growth experiment revealed cell division defects developing from 16 h, with cells having a swollen aspect and multiple nuclei, and this was more pronounced by 24 h. For 4-CF_3-phenyl substututed analogue FH9576, however, cells still looked normal at 16 h, although similar multi-nuclear cells could be observed by 24 h. These effect on cellular division would be consistent with incorporation into DNA, and disruption of the double helix structure, as DNA synthesis, at least, does not appear to be seriously impeded. Further research into the mode of action will be subject of follow-on studies.

CONCLUSION

In conclusion, optimisation of the published resorufin-based drug-sensitivity assay protocol allowed for the screening of several medium-sized or small compound libraries in this investigation. Through the use of this optimised protocol, we identified a series of 7-

substituted 7-deazaadenosine analogues that showed promising inhibitory activity against *T. vaginalis*. Of these, 18 compounds were more potent than metronidazole and displayed good-to-excellent levels of selectivity over HEK cells. A selection of these compounds was found to rapidly inhibit *T. vaginalis* growth and cause cell division defects at very low concentrations, especially the ribofuranoses. This may point to DNA fragmentation and chromosomal damage, but seems to exclude inhibition of DNA synthesis as a mode of action for these nucleoside analogues. Importantly, topical administration of lead compound TH1012 strongly inhibited *T. foetus* infection in mice.

Supplementary Material

Refer to Web version on PubMed Central for supplementary material.

Acknowledgements

REFERENCES

(1). Kissinger P (2015) *Trichomonas vaginalis*: a review of epidemiologic, clinical and treatment issues. BMC Infect. Dis 15, 307. [PubMed: 26242185]

(2). Bouchemal K, Bories C, and Loiseau PM (2017) Strategies for prevention and treatment of *Trichomonas vaginalis* infections. Clin. Microbiol. Rev 30 (3), 811–825. [PubMed: 28539504]

(3). Van Gerwen OT, and Muzny CA (2019) Recent advances in the epidemiology, diagnosis, and management of *Trichomonas vaginalis* infection. F1000Res 8, 1666.

(4). Menezes CB, Frasson AP, and Tasca T (2016) Trichomoniasis - are we giving the deserved attention to the most common non-viral sexually transmitted disease worldwide? Microb. Cell 3 (9), 404–19. [PubMed: 28357378]

(5). McClelland RS, Sangaré L, Hassan WM, Lavreys L, Mandaliya K, Kiarie J, Ndinya-Achola J, Jaoko W, and Baeten JM (2007) Infection with *Trichomonas vaginalis* increases the risk of HIV-1 acquisition. J. Infect. Dis 195 (5), 698–702. [PubMed: 17262712]

(6). Hirt RP, and Sherrard J (2015) *Trichomonas vaginalis* origins, molecular pathobiology and clinical considerations. Curr. Opin. Infect. Dis 28 (1), 72–79. [PubMed: 25485651]

(7). Stark JR, Judson G, Alderete JF, Mundodi V, Kucknoor AS, Giovannucci EL, Platz EA, Sutcliffe S, Fall K, Kurth T, Ma J, Stampfer MJ, and Mucci LA (2009) Prospective study of *Trichomonas vaginalis* infection and prostate cancer incidence and mortality: Physicians' Health Study. J. Natl. Cancer Inst 101 (20), 1406–1411. [PubMed: 19741211]

(8). Mitteregger D, Aberle SW, Makristathis A, Walochnik J, Brozek W, Marberger M, and Kramer G (2012) High detection rate of *Trichomonas vaginalis* in benign hyperplastic prostatic tissue. Microbiol. Immunol 201 (1), 113–116.

(9). Twu O, Dessí D, Vu A, Mercer F, Stevens GC, de Miguel N, Rappelli P, Cocco AR, Clubb RT, Fiori PL, and Johnson PJ (2014). *Trichomonas vaginalis* homolog of macrophage migration inhibitory factor induces prostate cell growth, invasiveness, and inflammatory responses. Proc. Natl. Acad. Sci. USA 111 (22), 8179–8184. [PubMed: 24843155]

(10). Cotch MF, Pastorek JG 2nd, Nugent RP, Hillier SL, Gibbs RS, Martin DH, Eschenbach DA, Edelman R, Carey JC, Regan JA, Krohn MA, Klebanoff MA, Rao AV, and Rhoads GG (1997) *Trichomonas vaginalis* associated with low birth weight and preterm delivery. The Vaginal Infections and Prematurity Study Group. Sex Transm. Dis 24 (6), 353–360. [PubMed: 9243743]

(11). Silver BJ, Guy RJ, Kaldor JM, Jamil MS, and Rumbold AR (2014) *Trichomonas vaginalis* as a cause of perinatal morbidity: a systematic review and meta-analysis. Sex Transm. Dis 41 (6), 369–76. [PubMed: 24825333]

(12). Schneider RE, Brown MT, Shiflett AM, Dyall SD, Hayes RD, Xie Y, Loo JA, and Johnson PJ (2011) The *Trichomonas vaginalis* hydrogenosomes proteome is highly reduced relative to mitochondria, yet complex compared with mitosomes. Int. J. Parasitol 41 (13–14), 1421–1434. [PubMed: 22079833]

(13). Brotman RM, Bradford LL, Conrad M, Gajer P, Ault K, Peralta L, Forney LJ, Carlton JM, Abdo Z, and Ravel J (2012) Association between *Trichomonas vaginalis* and vaginal bacterial community composition among reproductive-age women. Sex Transm. Dis 39 (10), 807–812. [PubMed: 23007708]

(14). Takao K, Rickhag M, Hegardt C, Ordesson S, and Persson L (2006) Induction of apoptotic cell death by putrescine. Int. J. Biochem. Cell Biol 38 (4), 621–628. [PubMed: 16406751]

(15). Rendon-Maldonado JG, Espinosa-Cantellano M, Gonzalez-Robles A, and Martinez-Palomo A (1998) *Trichomonas vaginalis*: In vitro phagocytosis of lactobacilli, vaginal epithelial cells, leukocytes, and erythrocytes. Exp. Parasitol 89 (2), 241–250. [PubMed: 9635448]

(16). Ryu JS, Choi HK, Min DY, Ha SE, and Ahn MH (2001) Effect of iron on the virulence of *Trichomonas vaginalis*. J. Parasitol 87 (2), 457–465. [PubMed: 11318588]

(17). Secor WE (2012) *Trichomonas vaginalis*: treatment questions and challenges. Expert Rev. Anti Infect. Ther 10 (2), 107–109. [PubMed: 22339182]

(18). Leitsch D, Kolarich D, Binder M, Stadlmann J, Altmann F, and Duchêne M (2009) *Trichomonas vaginalis*: metronidazole and other nitroimidazole drugs are reduced by the flavin enzyme thioredoxin reductase and disrupt the cellular redox system. Implications for nitroimidazole toxicity and resistance. Mol. Microbiol 72 (2), 518–536. [PubMed: 19415801]

(19). Cudmore SL, Delgaty KL, Hayward-McClelland SF, Petrin DP, and Garber GE (2004) Treatment of infections caused by metronidazole-resistant *Trichomonas vaginalis*. Clin. Microbiol. Rev 17 (4), 783–793. [PubMed: 15489348]

(20). Seña AC, Bachmann LH, and Hobbs MM (2014) Persistent and recurrent *Trichomonas vaginalis* infections: epidemiology, treatment and management considerations. Expert Rev. Anti Infect. Ther 12 (6), 637–685.

(21). Alessio C, and Nyirjesy P (2019) Management of resistant trichomoniasis. Curr. Infect. Dis. Rep 21, 31. [PubMed: 31388764]

(22). Edwards T, Burke P, Smalley H, and Hobbs G (2016) *Trichomonas vaginalis*: Clinical relevance, pathogenicity and diagnosis. Crit. Rev. Microbiol 42 (3), 406–417. [PubMed: 25383648]

(23). King JB, Carter AC, Dai W, Lee JW, Kil YS, Du L, Helff SK, Cai S, Huddle BC, and Cichewicz RH (2019) Design and application of a high-throughput, high-content screening system for natural product inhibitors of the human parasite *Trichomonas vaginalis*. ACS Infect. Dis 5, 1456–1470. [PubMed: 31265248]

(24). Campos Aldrete ME, Salgado-Zamora H, Luna J, Meléndez E, and Meráz-Ríos MA (2005) A high-throughput colorimetric and fluorometric microassay for the evaluation of nitroimidazole derivatives anti-trichomonas activity. Toxicol. In Vitro 19, 1045–1050. [PubMed: 15963680]

(25). Ibáñez Escribano A, Meneses Marcel A, Machado Tugores Y, Nogal Ruiz JJ, Arán Redó VJ, Escario García-Trevijano JA, and Gómez Barrio A (2012) Validation of a modified fluorimetric assay for the screening of trichomonacidal drugs. Mem Inst. Oswaldo Cruz 107, 637–643. [PubMed: 22850954]

(26). Natto MJ, Savioli F, Quashie NB, Dardonville C, Rodenko B, and De Koning HP (2012) Validation of novel fluorescence assays for the routine screening of drug susceptibilities of *Trichomonas vaginalis*. J. Antimicrob. Chemother 67, 933–943. [PubMed: 22258922]

(27). Natto MJ, Eze AA, and De Koning HP (2015) Protocols for the routine screening of drug sensitivity in the human parasite *Trichomonas vaginalis*. Methods Mol. Biol 1263, 103–110. [PubMed: 25618339]

(28). Hulpia F, Van Hecke K, Franca da Silva C, da Gama Jaen Batista D, Maes L, Caljon G, de Nazare CSM, and Van Calenbergh S (2018) Discovery of novel 7-aryl 7-deazapurine 3'-deoxy-

ribofuranosyl nucleosides with potent activity against *Trypanosoma cruzi*. J. Med. Chem 61, 9287–9300. [PubMed: 30234983]

(29). Hulpia F, Mabille D, Campagnaro GD, Schumann G, Maes L, Roditi I, Hofer A, De Koning HP, Galjon G, and Van Calenbergh S (2019) Combining tubercidin and cordycepin scaffolds results in highly active candidates to treat late-stage sleeping sickness. Nat. Commun 10, 5564. [PubMed: 31804484]

(30). Hulpia F, Campagnaro GD, Scortichini M, Van Hecke K, Maes L, De Koning HP, Caljon G, and Van Calenbergh S (2019) Revisiting tubercidin against kinetoplastid parasites: aromatic substitutions at position 7 improve activity and reduce toxicity. Eur. J. Med. Chem 164, 689–705. [PubMed: 30677668]

(31). Czekanska EM (2011) Assessment of cell Proliferation with resazurin-based fluorescent dye. Methods Mol. Biol 740, 27–32. [PubMed: 21468965]

(32). Schindelin J, Arganda-Carreras I, Frise E, Kaynig V, Longair M, Pietzsch T, Preibisch S, Rueden C, Saalfeld S, Schmid B, Tinevez JY, White DJ, Hartenstein V, Eliceiri K, Tomancak P, and Cardona A (2012) Fiji: An Open-Source Platform for Biological-Image Analysis. Nat. Methods 9 (7), 676–82. [PubMed: 22743772]

(33). Cobo ER, Eckmann L, and Corbeil LB (2011) Murine models of vaginal trichomonad infections. Am. J. Trop. Med. Hyg 85 (4), 667–673. [PubMed: 21976570]

(34). Abdellatif KRA, Elshemy HAH, and Azoz AA (2015) 1-(4-Methane(amino)sulfonylphenyl)-3-(4-substituted-phenyl)-5-(4-trifluoromethylphenyl)-1H-2-pyrazolines/pyrazoles as potential anti-inflammatory agents. Bioorg. Chem 63, 13–23. [PubMed: 26398140]

(35). Abdelatif KRA, Abdelgawad MA, Elshemy HAH, and Kahk NM (2016) Design and synthesis of certain novel bicoumarin derivatives as anticancer agents. Der Pharm. Chem 8 (3), 13–19.

(36). Abdelatif KRA, Abdelgawad MA, Elshemy HAH, Kahk NM, and El Amir DM (2017) Design, synthesis, antioxidant and anticancer activity of new coumarin derivatives linked with thiazole, isoxazole or pyrazole moiety. Lett. Drug Des. Disc 14 (7), 773–781.

(37). Abdellatif KR, Abdelgawad MA, Labib MB, and Zidan TH (2015) Synthesis, cyclooxygenase inhibition, anti-inflammatory evaluation and ulcerogenic liability of novel triarylpyrazoline derivatives as selective COX-2 inhibitors. Bioorg. Med. Chem. Lett 25 (24), 5787–5791. [PubMed: 26546221]

(38). Nnadi CO, Ebiloma GU, Black JA, Nwodo NJ, Lemgruber L, Schmidt TJ, and De Koning HP (2019) Potent antitrypanosomal activities of 3-aminosteroids against African trypanosomes: investigation of cellular effects and of cross-resistance with existing drugs. Molecules 24, 268.

(39). Alzahrani KJ, Matyugina ES, Khandazhinskaya AL, Kochetkov SN, Seley-Radtke KL, and De Koning HP (2017) Evaluation of the antiprotozoan properties of 5'-norcarbocyclic pyrimidine nucleosides. Bioorg. Med. Chem. Lett 27, 3081–3086. [PubMed: 28571825]

(40). Khandazhinskaya AL, Matyugina ES, Solyev PN, Wilkinson M, Buckheit KW, Buckheit RW Jr, Chernousova LN, Smirnova TG, Andreevskaya SN, Alzahrani KJ, Natto MJ, Kochetkov SN, De Koning HP, and Seley-Radtke KL (2019) Investigation of 5'-norcarbocyclic nucleoside analogues as antiprotozoal and antibacterial agents. Molecules 24, 3433.

(41). Baell JB, and Holloway GA (2010) New substructure filters for removal of pan assay interference compounds (PAINS) from screening libraries and for their exclusion in bioassays. J. Med. Chem 53 (7), 2719–2740. [PubMed: 20131845]

(42). Baell J, and Walters MA (2014) Chemistry: Chemical con artists foil drug discovery. Nature 513 (7519), 481–483. [PubMed: 25254460]

(43). Abraham MC, Desjardins M, Filion L, and Garber G (1996) Inducible immunity to *Trichomonas vaginalis* in a mouse model of vaginal infection. Infect. Immun 64, 3571–3575. [PubMed: 8751901]

(44). Meysick KC, and Garber GE (1992) Interactions between *Trichomonas vaginalis* and vaginal flora in a mouse model. J. Parasitol 78 (1), 157–160. [PubMed: 1310732]

(45). Shokar A, Au A, An SH, Tong E, Garza G, Zayas J, Wnuk SF, and Land KM (2012) S-Adenosylhomocysteine hydrolase of the protozoan parasite Trichomonas vaginalis: potent

inhibitory activity of 9-(2-deoxy-2-fluoro-β,D-arabinofuranosyl)adenine. Bioorg. Med. Chem. Lett 22 (12), 4203–4205. [PubMed: 22579483]

(46). Zang Y, Wang W-H, Wu S,-W, Ealick SE, and Wang CC (2005) Identification of a subversive substrate of *Trichomonas vaginalis* Purine Nucleoside Phosphorylase and the crystal structure of the enzyme-substrate complex. J. Biol. Chem 280, 22318–22325. [PubMed: 15817485]

(47). Harris DI, Beechey RB, Linstead D, and Barrett J (1988) Nucleoside uptake by *Trichomonas vaginalis*. Mol. Biochem. Parasitol 29 (2–3), 105–116. [PubMed: 2457803]

(48). De Koning HP, Bridges DJ, and Burchmore R (2005) Purine transporters of protozoa: from biology to therapy. FEMS Microbiol. Rev 29, 987–1020. [PubMed: 16040150]

(49). Munagala NR, and Wang CC (2003) Adenosine is the primary precursor of all purine nucleotides in *Trichomonas vaginalis*. Mol. Biochem. Parasitol 127 (2), 143–149. [PubMed: 12672523]
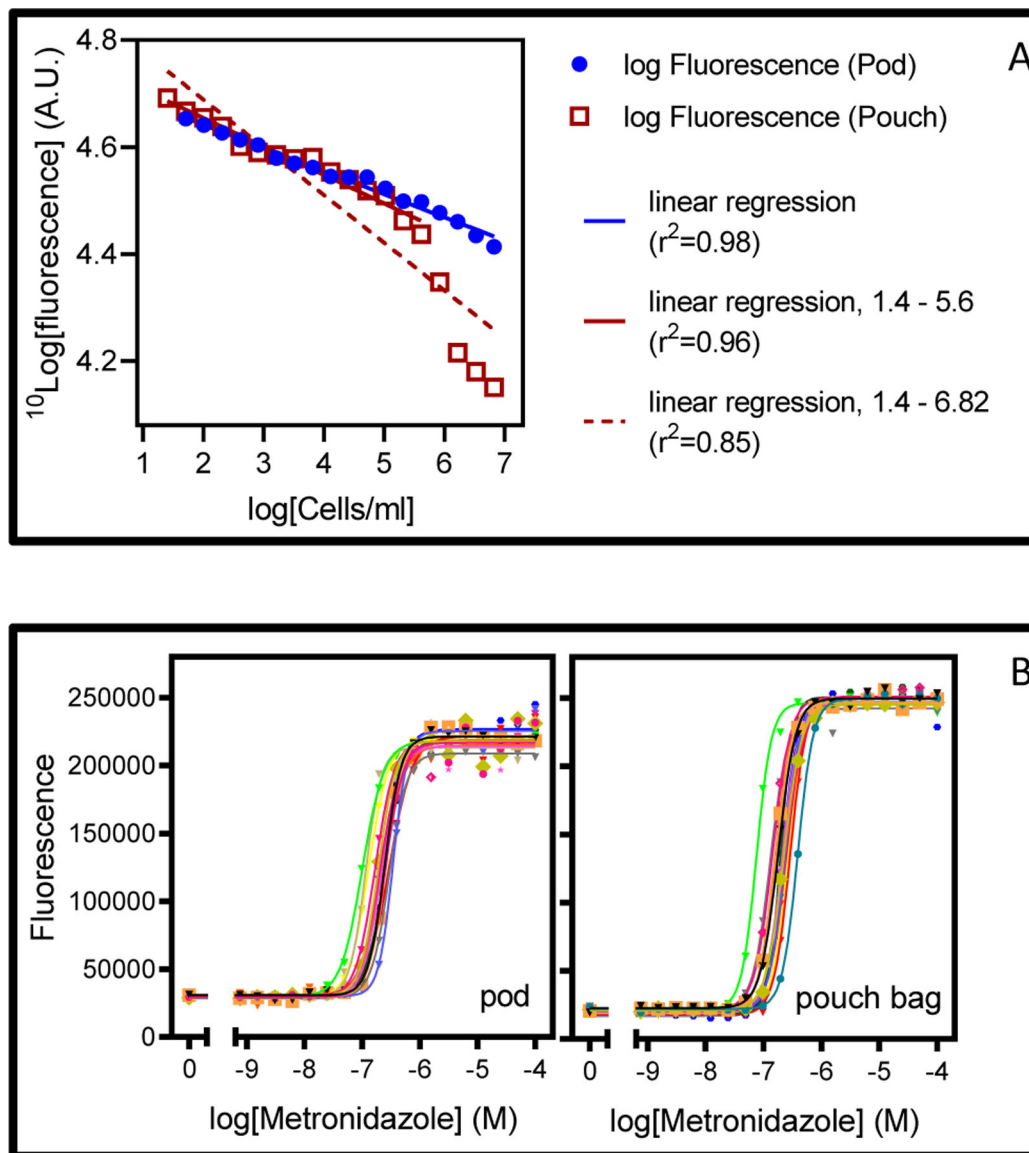
Figure 1.
A. Resorufin assay cell dilution with in-pod incubation (blue circles) or using BD pouch bags (brown open squares). Lines were plotted using linear regression in Prism 8.3 (GraphPad), yielding the indicated correlation coefficients; the slopes of both lines was highly significantly non-zero (P<0.0001). The dashed brown line also deviated highly significantly from linearity (P<0.0001). **B**. Fluorescence readout for resorufin assay with in-pod incubation (left-hand panel) or using BD pouch bags (right-hand panel). Each panel shows 16 separate dose-response curves for metronidazole starting at 100 μM. Sigmoid curves with variable slopes were plotted, and EC_{50} values determined using Prism 8.3.

Figure 2.
Structures of 7-deazaadenosine nucleoside analogues included in the *T. vaginalis* screening set.

Figure 3.
(**A**) Structures of ribofuranose and 3'-deoxyribofuranose nucleoside analogues; (**B**) Structures of di-substituted phenyl analogues.
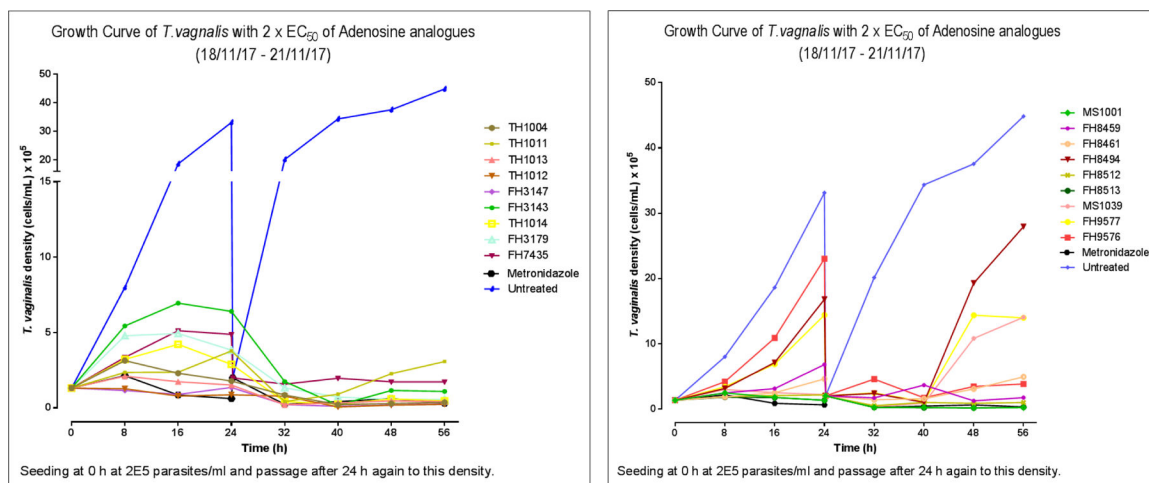
Figure 4.
Growth curves of T. vaginalis trophozoites incubated with selected hit adenosine analogue compounds at $2 \times$ the EC50 value for a duration of 56 h. Cultures were seeded at 1.35×105 cells/mL and after 24 h were again passaged to the same density, in the continuous presence of the test compound. (A) Matched pairs of ribofuranosyl (closed symbols and solid lines) and 3′-deoxy ribofuranosyl compounds (open symbols, dashed lines). (B) Exploration of the nature of the 7-(4-phenyl) position of ribofuranosyl (closed symbols and solid lines) and 3′-deoxy ribofuranosyl compounds (open symbols, dashed lines) on the growth of T. vaginalis. The data presented are the average and SD of triplicate determinations for each condition, indicating cell counts from three different cultures grown in parallel in multiwell plates. Error bars mostly fall within the symbol.
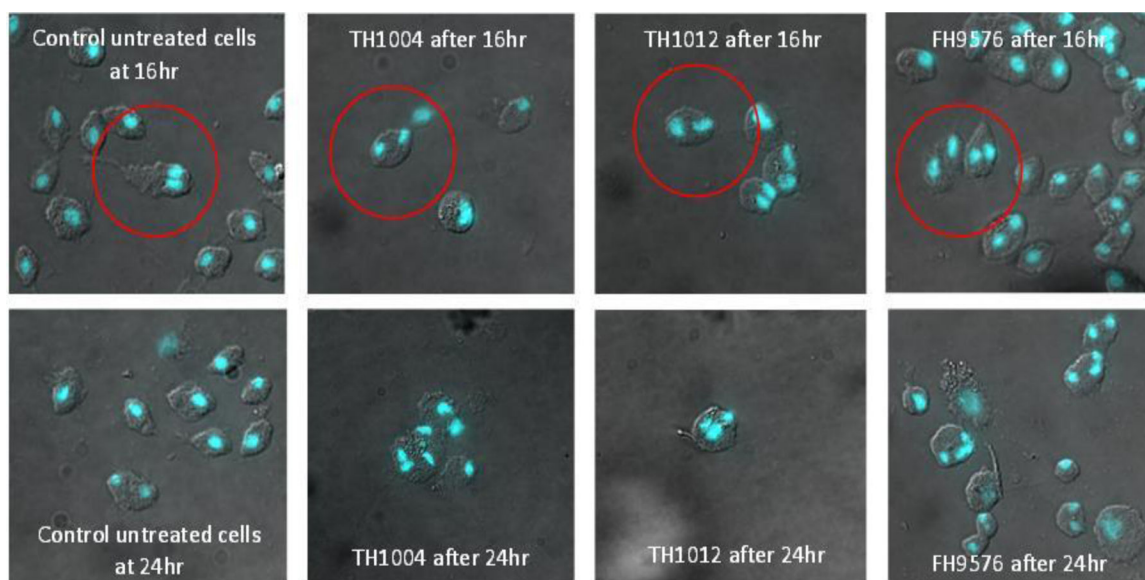
Figure 5.
DAPI staining (blue fluorescence) on differential interference contrast imaging showing a comparison of cell structures after 16- and 24-h continuous incubation with three adenosine analogue test compounds. TH1004, TH1012 and FH9576 were selected as it can be seen from the growth curve that each compound causes cell growth inhibition at different time points and so it was thought that this could suggest differing mechanisms of action. Circled in red are cells believed to be undergoing G2-phase division at 16-h (circled for comparison with treatment-induced multinucleate cells seen at 24 h).

Compound ID	*T. vaginalis* F1623		*T. foetus* D1	
	pEC$_{50}$	EC$_{50}$ (µM)	pEC$_{50}$	EC$_{50}$ (µM)
TH1012	6.75 ± 0.20	0.18	4.86 ± 0.11	13.92
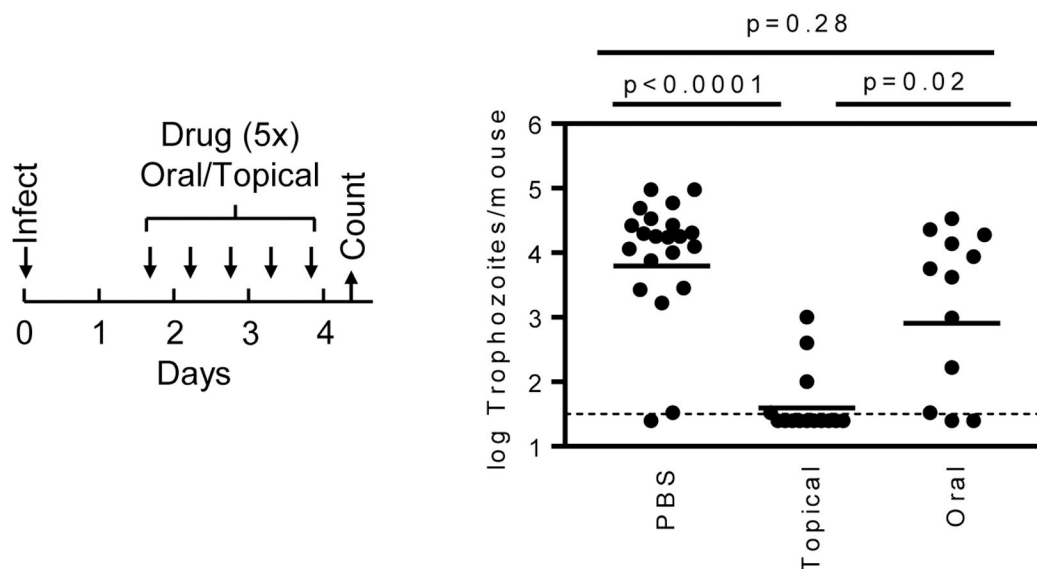
Figure 6.

In vivo efficacy of TH1012 in a mouse model of *T. foetus*. Weanling BALB/c mice were inoculated intravaginally with *T. foetus* trophozoites. After one day, mice were treated five times TH1012 orally (i.e. 5×25 mg/kg) or intravaginally (Topical, 1%). Infected mice given PBS served as the control. Live trophozoites were enumerated in vaginal washes on day 4 (bars are geometric means, circles show individual mice; n=6–17 mice/group; Statistics were evaluated by Kruskal-Wallis with Dunn's post-hoc test or Mann-Whitney test; ns, not significant). The dashed line depicts the detection limit of the assay.

Table 1.

EC$_{50}$ values of 7-substituted 7-deazaadenosine analogues against T. vaginalis and HEK cells.

Compound ID	7-position subst.	EC$_{50}$ T. vaginalis (μM)	EC$_{50}$ HEK (μM)	S.I.
ribofuranoses				
TH1004	Ph	0.44 ± 0.059	>200	>465
TH1011	4Me-Ph	0.068 ± 0.009	>200	>3333
TH1012	4Cl-Ph	0.035 ± 0.007	>200	>6667
TH1013	4MeO-Ph	0.21 ± 0.04	>200	>952
FH3147	3,4diCl-Ph	0.029 ± 0.003	>200	>10,000
MS1001	4F-Ph	0.11 ± 0.034	>200	>1818
FH11704	4CF$_3$-Ph	0.18 ± 0.05	>200	>313
FH10715	4CF$_3$O-Ph	1.99 ± 0.26	>200	>23.3
FH11702	4Et-Ph	0.19 ± 0.037	>200	>115
FH13828	4cyano-Ph	2.16 ± 0.03	>200	>30
FH13832	4carboxamido-Ph	27.4 ± 0.49	ND	--
FH13834	4(Me-sulfonyl)-Ph	74.2 ± 0.8	ND	--
FH13833	4hydroxy-Ph	0.15 ± 0.03	>200	>158
FH8459	3Cl-Ph	0.24 ± 0.048	>200	>833
FH13817	3Me-Ph	0.77 ± 0.019	>200	>83
FH13826	3F-Ph	1.52 ± 0.029	>200	>32
FH13835	2Cl-Ph	9.6 ± 0.30	ND	--
FH13821	2Me-Ph	9.00 ± 0.31	>200	>22
FH7435	2F-Ph	0.21 ± 0.068	>200	>952
FH11705	3Me,4Cl-Ph	0.14 ± 0.014	>200	>1429
FH13827	3-CF$_3$,4Cl-Ph	12.7 ± 0.47	84.2 ± 3.7	7
FH10714	3F,4Cl-Ph	0.12 ± 0.009	ND	--
FH13823	2F, 4Cl-Ph	0.077 ± 0.013	>200	>2597
FH8460	3,5-diCl-Ph	1.99 ± 0.56	>200	>101
FH13820	3,4diMe-Ph	0.43 ± 0.008	>200	>465
FH11703	3Cl,4Me-Ph	0.058 ± 0.077	>200	>3448
FH13829	3F,4Me-Ph	0.36 ± 0.02	>200	>556
FH13824	2F,4Me-Ph	0.23 ± 0.02	>200	>870
FH11706	3,4diF-Ph	0.25 ± 0.025	>200	>800
FH11707	3Cl,4F-Ph	0.34 ± 0.062	>200	>588
FH13825	3Cl,4CF$_3$-Ph	0.37 ± 0.01	>200	>541
FH13830	3Me,5Cl-Ph	23.5 ± 0.41	ND	--
FH8461	naphtyl	0.58 ± 0.101	147 ± 22	345
FH4185	3-pyridyl	8.54 ± 0.962	ND	--
FH4184	5-pyrimidyl	9.80 ± 0.483	ND	--

Compound ID	7-position subst.	EC$_{50}$ *T. vaginalis* (μM)	EC$_{50}$ HEK (μM)	S.I.
FH3179	2-pyridazinyl	0.74 ± 0.131	ND	--
FH3182	N1-methyl-4-imidazolyl	2.10 ± 0.336	ND	--
MS1039	5-Cl-2-pyrimidyl	0.86 ± 0.136	ND	--
MS1016	4-Me-2-pyrimidyl	2.80 ± 0.478	ND	--
MS1017	2-quinolinyl	2.27 ± 0.272	ND	--
3'-deoxyfuranoses				
FH8480	Ph	8.3 ± 0.97	ND	--
FH8481	4Me-Ph	1.55 ± 0.04	>200	>129
FH8512	4Cl-Ph	0.17 ± 0.044	>200	>1176
FH8494	4MeO-Ph	0.73 ± 0.093	>200	>274
FH8513	3,4diCl-Ph	0.33 ± 0.115	>200	>606
FH10680	4F-Ph	2.00 ± 0.18	>200	>100
FH9576	4CF$_3$-Ph	0.26 ± 0.075	148 ± 22	568
FH9577	4CF$_3$O-Ph	0.79 ± 0.292	ND	--
FH10647	4Et-Ph	0.79 ± 0.047	133 ± 2	169
FH10641	3Cl-Ph	3.67 ± 0.39	>200	>54
FH10639	3Me-Ph	14.21 ± 1.20	ND	--
FH9574	4*i*Pr-Ph	1.20 ± 0.484	94 ± 9	79
FH9582	4nitro-Ph	1.34 ± 0.216	>200	>149
FH10667	cyclohexen-2-yl	49.0 ± 4.68	ND	--
FH10669	cyclohexyl	42.8 ± 2.18	ND	--
FH10640	3CF$_3$-Ph	72.63 ± 22.31	ND	--
FH10648	3Me,4Cl-Ph	0.74 ± 0.058	146 ± 13	198
FH10683	3F,4Cl	1.57 ± 0.039	151 ± 1	96
FH10642	3,5diCl-Ph	9.48 ± 1.06	ND	--
FH10653	3,4Me-Ph	4.07 ± 0.96	168 ± 19	41
FH10644	3Cl,4Me-Ph	0.42 ± 0.021	94 ± 9	225
FH10682	3,4diF-Ph	2.48 ± 0.094	>200	>81
FH10681	3Cl,4F-Ph	1.78 ± 0.21	>200	>112
FH10645	3Cl,4CH$_3$O-Ph	3.06 ± 0.41	>200	>65
FH9575	naphtyl	2.05 ± 0.253	44 ± 5	21
FH9581	2,4-diCl-Ph	1.62 ± 0.31	>200	>123
FH10649	3MeO,4Cl-Ph	1.75 ± 0.15	178 ± 6	>102
2'-deoxyfuranoses				
FH11708	Ph	1.56 ± 0.27	>200	>128
FH11709	4Me-Ph	0.65 ± 0.34	>200	>308

Compound ID	7-position subst.	EC$_{50}$ *T. vaginalis* (μM)	EC$_{50}$ HEK (μM)	S.I.
FH11711	4Cl-Ph	0.46 ± 0.13	>200	>435
FH11710	4MeO-Ph	1.41 ± 0.34	104 ± 14	142
FH11713	3,4diCl-Ph	0.42 ± 0.057	>200	>248
FH11712	4F-Ph	0.80 ± 0.086	>200	250
FH13822	3Cl,4Me-Ph	1.11 ± 0.05	112 ± 11	101

Ph, phenyl; ND, not determined; SI, Selectivity Index. All values are the average of at least 3 independent determinations and SD.